JOURNAL OF MATERIALS SCIENCE 25 (1990) 168–174

The nickel-rich corner of the Ni–Al–Ti system

P. WILLEMIN*, M. DURAND-CHARRE
Institut National Polytechnique de Grenoble, L.T.P.C.M.-E.N.S.E.E.G., BP 75 38402 Saint-Martin d'Hères, France

Liquid–solid equilibria were studied in the nickel-rich corner of the Ni–Al–Ti system, using a combination of several experimental techniques, essentially differential thermal analysis (DTA) and all usual techniques of characterization. A modified version of the DTA technique, quench-interrupted DTA, was employed in order to establish the solidification paths. A projection of the liquidus surface is proposed and the nature of the monovariant lines is defined. One result is the occurrence of a ternary peritectic reaction between γ, γ' and the liquid. Solid-state equilibria are determined for a temperature of 1250° C and the investigation has focused on the γ' solid phase field.

1. Introduction

The constitutional effects of alloying additions in superalloys are complex and involve many aspects. The promotion of γ' precipitates is the main requirement in order to improve high temperature strength and microstructural stability. The contribution of titanium for the enlargement of the γ' solid solution is well known. A typical example of a cast nickel base superalloy is IN-100 which contains almost 5 wt % titanium and about 5.5 wt % Al. Nevertheless additions of titanium are limited on account of its ability to induce high porosity in castings. In recent alloys, the role of titanium as a γ' stabilizer must be shared with other elements such as tantalum.

From a more theoretical point of view, the Ni–Al–Ti system remains a reference for discussion of γ–γ' equilibria and crystallization paths and one of our aims is to obtain a good model of this system by thermodynamical calculations. Moreover, the development of *a priori* calculations of phase equilibria requires much data: data for binary systems and also for ternary or more complex systems since the formation of a ternary phase cannot be predicted from calculations involving binary data.

A few studies have been made on this system. Most of them concern solid-state equilibria. Manenc in 1959 [1] has shown the formation of metastable precipitates for compositions close to Ni_3Ti using a TEM replica technique. Taylor and Floyd [2] have determined isothermal sections for temperatures ranging between 750 and 1150° C. Mihalisin and Decker [3] have explained the mechanism for the precipitation of the η phase by TEM observations on long time annealed alloys. Mints *et al.* [4] have studied the section Ni_3Al–Ni_3Ti. In particular they measured the liquidus temperatures by thermal analysis. Recently, Nash and Liang [5] have determined an isothermal section at 900° C. They propose an outline of the liquidus projection from their results for solid–solid equilibria.

The purpose of the present investigation is to increase the amount of data in the γ–γ' field and, particularly, to establish the liquidus projection from the determination of the liquid–solid equilibria.

2. Experimental procedure

Master alloys were melted in a medium frequency induction furnace under controlled atmosphere using high purity charge materials (> 99.95%). Intermediate compositions were prepared from these alloys by button melting in an argon-arc furnace. In all, a total of about 60 alloys were studied. The range of compositions was 0 to 30 at. % Al, 0 to 30 at. % Ti, Ni balance. In order to reduce segregations resulting from solidification, all the ingots were homogenized for 24 h at 1250° C. In the case of as-cast alloys presenting Ni_3Ti needles, the annealing time was increased up to 130 h.

The phase transformation temperatures were determined by differential thermal analysis (DTA) on specimens of about 2 g. Heating and cooling were carried out under argon at a rate of 300° C h^{-1}. The range of temperature variation is rather small, so these temperatures alone are not sufficient to determine the different fields for each primary phase. The investigation has to be completed by careful phase identification and analysis. Another method employed was to monitor solidification occurring under controlled conditions in the DTA furnace and to quench the specimen at a precise moment, either on attainment of the liquidus surface or at the appearance of a eutectic. This method (QDTA) in which the solid–liquid interface configuration is frozen in by rapid cooling enables the solidification sequence to be determined. In effect, the information concerning the composition of the first solid (dendrite core) and that of the liquid determines a tie-line which indicates the direction of the crystallization path. Complementary information is obtained by the analysis of minor phases located in the

Present address: Research Department, IMPHY S.A 58160 Imphy, France.

0022–2461/90 $03.00 + .12 © *1990 Chapman and Hall Ltd.*

interdendritic groove. Solvus temperatures were determined either by DTA experiments using 6 g samples without a crucible as previously described [6], or by phase analyses on annealed samples.

Optical micrography was carried out on polished sections etched in aqua regia reagent.

Phase analyses were conducted with an electron-microprobe, using an accelerating voltage of 10 kV for aluminium, 15 kV for titanium and 20 kV for nickel, with the application of a ZAF correction program (atomic number, absorption and fluorescence). Phases present in the form of fine particles, were analysed semiquantitatively on a scanning electron microscope (SEM) equipped with a solid-state detector.

X-ray diffraction was used to identify phases, mostly on powdered samples, particularly for determining lattice parameters. The measurements of lattice parameters were made on samples which had been annealed at 1250° C and then quenched. Investigations were also performed using electron diffraction on thin foils.

3. Results

3.1. Phase equilibria

Five phases have been identified within the triangle Ni–NiAl–Ni_3Ti γ, γ', β, η and H. The crystal structures are given in Table I. The lattice parameters indicated include both measurements obtained in the present study and values from the literature for the β and H phases [5, 7, 8].

The phase transformation temperatures and the phases which may appear during solidification are listed in Table II. The latter indicates all the phases detected in the samples, either after a quench or after a slower rate of freezing during the DTA experiments. As the crystallization paths depend on the rate of freezing, it must be specified that the temperatures correspond to a 300° C h^{-1} rate of cooling. In addition, sometimes the peaks are broad and include two different thermal accidents that cannot be deconvoluted.

The liquidus surface in the primary γ solid-solution phase field has been represented by a second-order polynomial function of the atomic concentrations of each constituent element. The coefficients in this equation were determined by a least squares fitting

TABLE II Transformation temperatures determined by DTA experiments at a cooling rate of 300° C h^{-1} and phases formed during crystallization in the order of their appearance

Composition		Transformation temperatures (°C)			Phases formed in order of appearance
Al (at.%)	Ti (at.%)				
3.1	0.9	1445			γ
3.05	1.75	1436			γ
6.52	1.94	1430			γ
16	2	1400			γ, γ'
14	2	1404			γ, γ'
19.14	2.05	1380	1353		γ, γ'
14	4	1392	1360		γ, γ'
5.55	4.92	1404	1292		γ
14	6	1368	1348		γ, γ', η
12	6	1380	1346		γ, γ', η
4.36	6.55	1390			γ
9.86	8.86	1353	1336		γ, γ', η
5.32	8.93	1368			γ
7.05	10.63	1342	1317		γ, γ'
8.01	12.05	1334	1317		γ, γ', η
1.98	14.32	1335	1315	1305	γ, η
4.14	14.46	1322	1315		γ, η, γ'
5.41	15.27	1322	1300		γ, η, γ'
6	16	1317	1300		γ, γ', η
3.21	16.63	1320	1314		γ, η
3	19	1327	1310		γ, η, γ'
24.12	1.99	1375			γ'
17.92	3.96	1368	1356		γ', γ
18.09	5.39	1373			γ', γ
18.3	5.92	1373	1356		γ'
16	6	1356			γ', γ
18.24	7.93	1374			γ', β
14	8	1354	1346		γ', γ
22.67	8.21	1346			γ', β
16.99	9.77	1360	1315		γ', β
16.9	10	1360	1315		γ', β
12	10	1340			γ', γ, η
9.25	13.94	1346	1317		γ', γ, η
10	15	1363	1324		γ', η
10.14	15.24	1363	1324		γ', η
6.58	16.39	1342	1330	1312	γ', γ, η
20.3	20	1360			γ'
5.52	20.13	1369	1268		η, γ', H
10.14	16.93	1345	1270		η, γ', H
11.98	18.02	1332	1275		η, γ', H
7.97	23.59	1333	1265	1135	η, H
2	20	1317			η, γ, γ'
2	22	1380	1305		η, γ, γ'
8.11	18.13	1352	1270		η, γ', H
3.83	16.95	1348	1319		η, γ, γ'
18.5	16.28	1316	1277		β, γ', H

TABLE I Phases identified in the nickel-rich corner of Ni–Al–Ti system

Phases		Ni (γ)	Ni3Al (γ')	Ni_3Ti (η)	NiAl (β)	Ni_2AlTi (H)
Type		Cu	Cu_3Au	Ni_3Ti	CsCl	$AlCu_2Mn$
Space group		Fd3m	P m3m	P 63 mmc	P m3m	F m3m
Struck.-Bericht		A1	L1	D0	B2	L2
Al (at.%)	Ti (at.%)					
25	0		a = 0.3567 (present results)			
0	14	a = 0.356 (present results)		a = 0.510, c = 0.830 (present results)		
biphased						
28	24					a = 0.589 [5]
10.1	15.2		a = 0.3590 (present results)			
18.3	5.9		a = 0.3580 (present results)			
36.5	0				a = 0.2870 [8]	

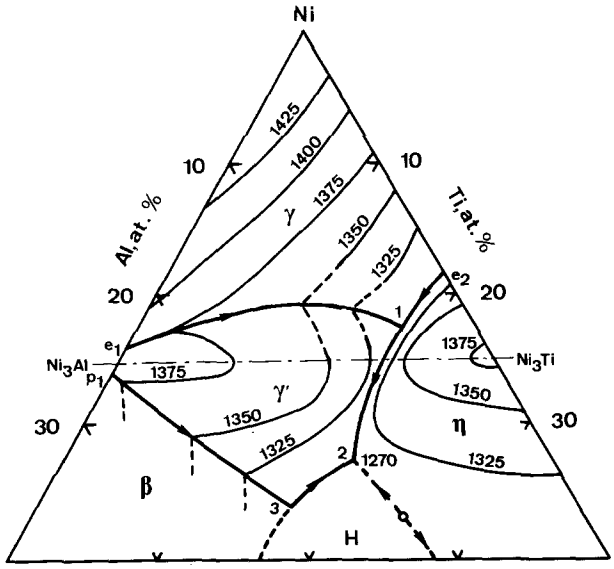

Figure 1 Projection of the liquidus surface with isothermal lines.

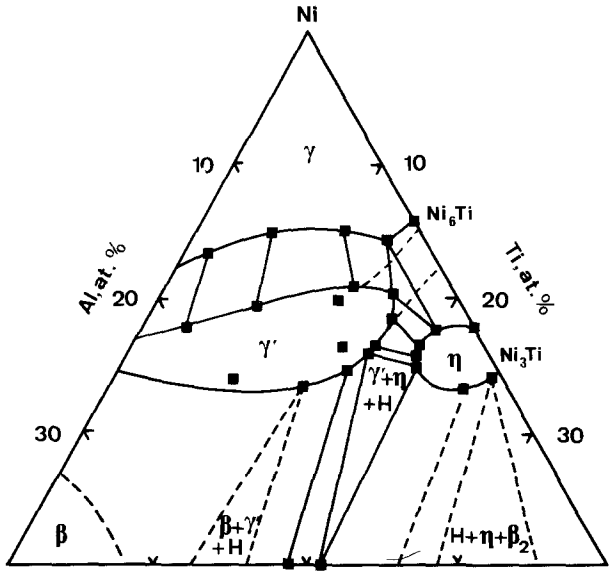

Figure 3 Isothermal section at 1250° C.

technique, using 20 experimentally determined values in the ternary field. The following expression was obtained.

$$T = 1455 + 0.6935x_{Al} - 10.7221x_{Ti} - 0.17x_{Al}^2 - 0.08x_{Al}x_{Ti} + 0.16x_{Ti}^2 \quad (1)$$

where T is the temperature (° C) and x_i the at. % content of i. The discrepancy between the experimental values and those calculated from the above relation is less than 7° C, which is the order of magnitude of the overall precision of the liquidus measurements.

Fig. 1 represents the projection of the liquidus surface showing isothermal and monovariant lines, together with the boundaries of each phase field. Three points 1, 2 and 3 indicate invariant ternary reactions involving three solid phases and the liquid. For points 1 and 3 the reaction is peritectic since the crystallization does not end there, while it is eutectic for point 2.

Fig. 2 shows the projections of the tie-lines established at the liquidus temperature for each composition.

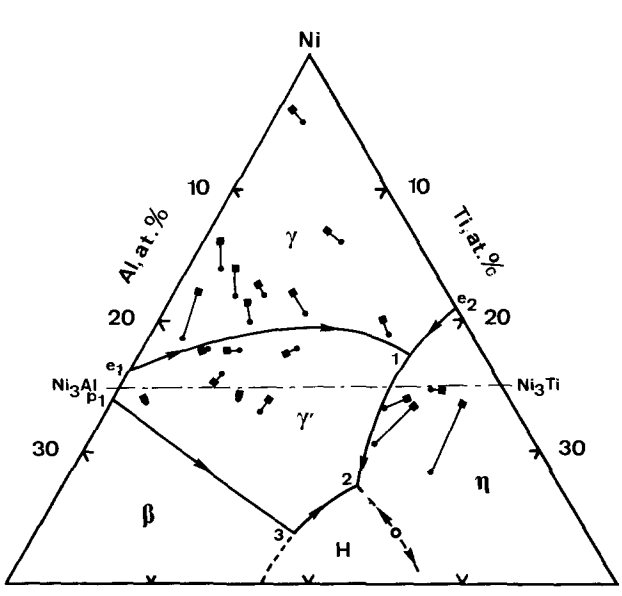

Figure 2 Projection of tie-lines at the liquidus temperature. The points indicate the liquid composition while the squares indicate the solid composition.

Fig. 3 represents an isothermal section at 1250° C. Figs 4a, b and c represent vertical sections which illustrate the variation of the γ/γ' solid-state equilibria with the temperature.

3.2. Microstructures

Many different kinds of morphologies were found for γ in the relationship with the initial composition of the alloy the rate of freezing and the rate of cooling and have been presented elsewhere [7].

In the case of titanium-rich alloys with compositions close to the monovariant line, the microstructures change markedly during high temperature exposure, the variations being more complex than a single precipitation reaction. This change is illustrated by the example of an alloy containing 12 at. % Ti and 8 at. % Al. Samples were quenched at different stages of a 300° C h^{-1} programmed cooling cycle performed in the DTA apparatus. Fig. 5a shows that, when quenching is carried out at the liquidus temperature, the primary γ' dendrites are perfectly homogeneous. Figs 5b and c correspond to the same alloy quenched respectively from 5° C and 20° C below the liquidus. The γ' has undergone a transformation, with rejection of the γ phase. This transformation ultimately leads to the formation of spherical pockets whose appearance suggests partial remelting. These pockets appear dark in Fig. 6a. In rapidly cooled samples they contain a dense precipitation of hyperfine γ' particles, whereas the latter have a coarser, dendritic morphology in slowly cooled specimens (Fig. 6b).

4. Discussion and conclusions

4.1. Phase equilibria

The extent of the γ' field on the liquidus surface was found to be very large, greater than previously described. In particular, in the direction of high nickel content, the monovariant line is curved. This curvature reveals a strong interaction between aluminium and titanium. The same observation was made in the Ni–Al–Ta system for aluminium and tantalum [6]. The direction of the tie-lines changes for nickel contents higher and lower than 75 at. % in the range of

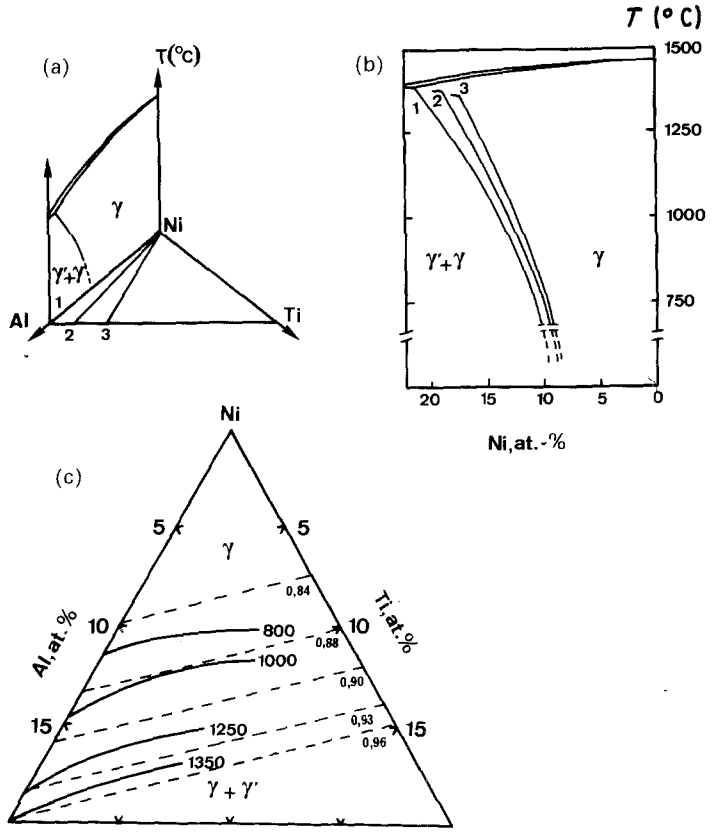

Figure 4 γ/γ' phase fields for different Ti/Al contents. (a) Temperature plotted against composition diagram; (b) space representation; (c) projection of isothermal phase boundaries at different temperatures and, with broken lines, isoparametric M_d lines.

titanium contents comprised between 5 and 15 at. %. The shape of the liquidus surface is that of a ridge along the 75 at. % Ni section which vanishes for higher titanium content. At the top of this ridge, for about 5 to 10 at. % Ti, the tie-lines are very short indicating that the liquid and the solid have similar compositions. Although it was not possible to establish evidence for actual congruency of γ' in a ternary range of compositions, this suggests that solidification without segregation could be performed rather easily for compositions at the top of the ridge, hence, facilitating the preparation of monocrystals.

The isothermal section presented in Fig. 3 is in good overall agreement with data from the literature. The large number of compositions investigated has enabled the phase boundaries to be defined more accurately. It then appears that the single-phase field of γ' is enlarged, indicating greater solubilities for aluminium and titanium respectively. The metastable precipitation of a γ' type structure in titanium-rich alloys has been extensively studied in both commercial alloys and in binary Ni–Ti alloys [7]. In this latter system, the composition of the precipitates appeared to be close to Ni_6Ti. Thus, the prolongation of the γ' field up to Ni_6Ti (Fig. 3) delimits the range of compositions for this metastable precipitation.

The extent of the γ' field has been illustrated by Guard and Westbrook for the system Ni–Al–X (X represents a transition element) on an isothermal section at 1150° C. This field has an oval shape orientated along two main directions depending on the nature of the X elements. For one family, which consists of niobium, vanadium, titanium [2] and tantalum [6], the boundary between γ' and β is a nickel iso-content line. It is interesting to consider this result in terms of the crystal structure of Ni_3Al which can be described as two cubic sublattices containing respectively nickel atoms and aluminium atoms. The X elements are disposed on either sublattice according to their bonding characteristics. Aluminium can be easily replaced by titanium, tantalum, niobium and also nickel, whereas nickel can be readily substituted only by cobalt. Iron and chromium can substitute in either sublattice. Vacant sites can occur in the aluminium sublattice. Time-of-flight atom probe experiments made by Blavette and Bostel [9] tend to corroborate this conclusion.

4.2. Lattice parameter of the γ' phase

In order to discuss the substitutional behaviour, we supplemented these observations with a compilation

TABLE III Lattice parameters of the τ' phase according to the composition of the alloys

a (nm)	Al (at.%)	Ti (at.%)	Reference
0.356 60	25.10	0.00	[2]
0.356 50	23.20	0.00	[2]
0.356 80	25.00	0.00	[2]
0.356 80	25.00	0.00	[10]
0.356 80	25.00	0.00	present results
0.356 70	25.90	0.00	[2]
0.357 00	26.40	0.00	[2]
0.357 30	18.80	4.60	[2]
0.358 00	20.00	5.00	[10]
0.357 70	19.40	5.80	[2]
0.358 00	18.30	5.92	Present results
0.358 30	15.50	9.90	[2]
0.358 21	13.40	10.00	[2]
0.358 90	15.00	10.00	[10]
0.358 61	11.90	12.40	[2]
0.359 06	9.60	14.80	[2]
0.358 90	10.60	15.00	[2]
0.359 00	10.14	15.24	Present results
0.358 98	11.00	15.50	[2]

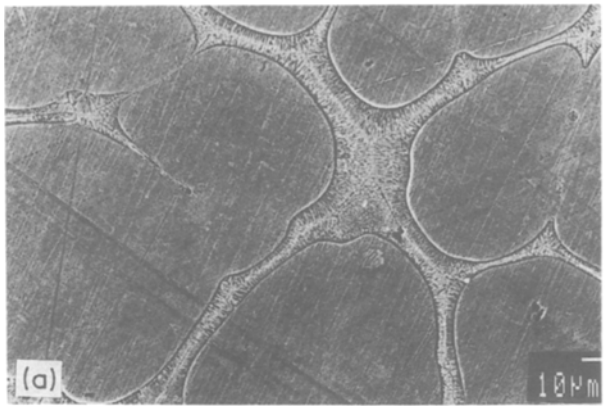

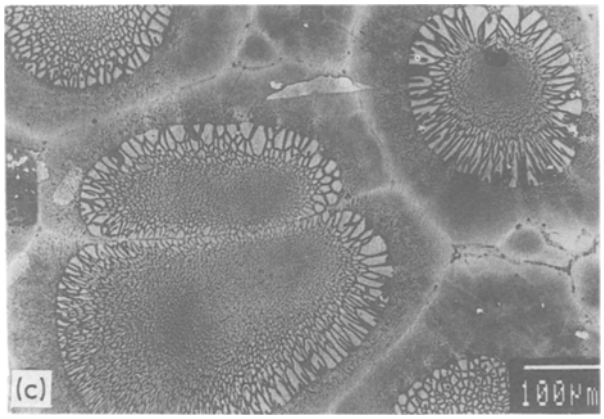

Figure 5 Electron micrographs of the alloy 8 at. % Al and 12 at. % Ti quenched at different stages of its freezing: (a) at the liquidus temperature, (b) 5° C below the liquidus temperature, (c) 20° C below the liquidus temperature.

of lattice parameters. Many studies have been devoted to the influence of additional elements on lattice parameter variation since such data is useful for predicting the mismatch between γ and γ' [2, 7, 10, 11]. We reported on a ternary diagram the compositions investigated (Fig. 7) and we represented the lattice parameter by two second-order and first-order polynomial functions of the atomic concentrations of aluminium and titanium. This treatment was possible for the system considered because the data are numerous (Table III) and also because temperature has little effect on the lattice parameter values. In effect, the order of variation is 0.5% between 850 and 1250° C, which may be neglected with respect to the alloying effect. In other systems such as Ni–Al–Ta the variation is larger and cannot be neglected. The relation is

$$a = 0.3568 + 0.4 \times 10^{-4}(x_{Al} - 25) + 1.9 \times 10^{-4} x_{Ti} \quad (2)$$

where a is the lattice parameter (nm) and x_i is the at. % content of i.

The discrepancy between the experimental and the calculated values is less than 0.12%. Assuming that an average overall uncertainty of lattice measurements may be estimated at 1.6×10^{-4} nm, the representation is justified. Ochiai *et al.* [12] published a compilation concerning lattice parameter variation in Ni_3Al (γ') solid solutions with additions of transition metals evaluated both with their experimental results and previously published data. They propose the following law for the variation of lattice parameter

$$a = 0.357 + 2.5 \times 10^{-4} \times \text{at. \% Ti} \quad (3)$$

which agrees quite well with our results. In fact Equation 2 indicates the influence of the substituting element only in one direction in the ternary field.

Fig. 7 presents the calculated isoparametric lines. It can be seen that one of these lines coincides with the limit for solubility of γ' phase at 1250° C and, moreover, that this limit is parallel to the titanium axis. As the atomic sizes of titanium and nickel are almost equal, no steric effect is induced by substitution between them. However, similar results are obtained with

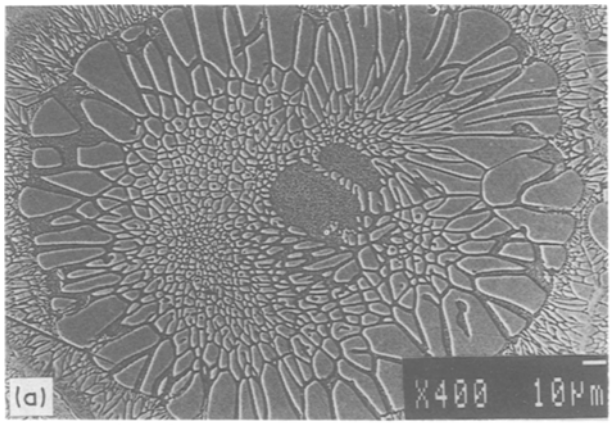

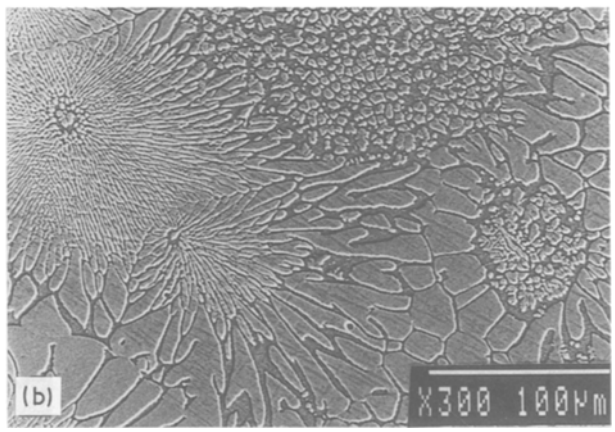

Figure 6 Electron micrographs of the alloy 8 at. % Al and 12 at. % Ti (a) quenched 40° C below the liquidus temperature, (b) cooled at a rate of 300° C h^{-1}.

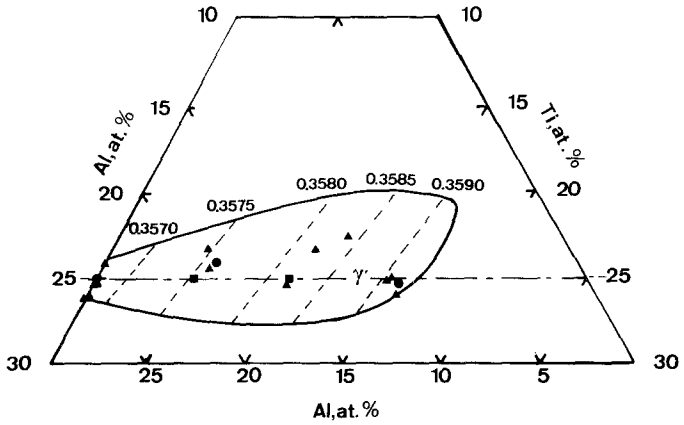

Figure 7 Isoparametric lines for the γ' phase in the ternary field. ▲ corresponds to [2], ■ corresponds to [10] and ○ to our work (measurements made on samples annealed at 1250° C and then quenched).

tantalum substitution [7]. This suggests that, in fact, the effect involved is electronic.

4.3. M_d new Phacomp parameter

Several attempts have been made to take into account the electronic effect in order to predict the occurrence or the limits of solubility of the phases. The most recent one [13] is the New Phacomp model which introduces a parameter M_d which represents an average level of the energies of orbitals for transition metals. The iso M_d lines are reported in Fig. 4c. As the model is a rather simple linear relationship, they are straight lines. Thus a strong chemical interaction, inducing curved limits, cannot be taken into account.

4.4. Equilibria along the γ/γ' monovariant line

In the Ni–Al–Ti ternary system, for low titanium concentrations, the equilibrium between γ and γ' liquid is of a monovariant eutectic nature. As titanium content increases, the equilibrium changes and becomes peritectic. This signifies that a titanium-rich alloy whose composition lies in the primary γ field can end solidification with the formation of β phase, since the solidification path can cross the peritectic line (Fig. 8).

The formation of a liquid by remelting γ' can be explained by the γ–γ' configuration proposed in Fig. 9, based on analyses of the remelted zones and of the adjacent γ'. The first stage represents the homogeneous solid (point M), while the second one (tie-lines 3), at a temperature a few degrees lower, corresponds to the decreasing solubility of nickel, and especially titanium, in γ', leading to the formation of a γ network in the primary γ' dendrites. The third stage (tie-lines 4) represents the appearance of a three-phase equilibrium when the γ solubility limit is reached.

The system Ni–Al–Ti constitutes a good approach for superalloys, thus our investigation has focused on the nickel-rich corner of the ternary field of this system. We have clearly illustrated the competition between titanium and aluminium in forming A_3B type phases with nickel. We established that specific morphologies were linked with peritectic and even metatectic nature of the γ–γ'-liquid reactions.

Acknowledgements

This work was performed in the scope of the French Scientific Group "Superalloys for single crystal turbine blade materials" with the financial support of the "Direction des Recherches, Etudes et Techniques".

References

1. J. MANENC, *Acta Metall.* 7 (1959) 124.
2. A. TAYLOR and R. W. FLOYD, *J. Inst. Met.* **81** (1952–53) 25.
3. J. R. MIHALISIN and R. F. DECKER, *Trans. Met. Soc. AIME* **218** (1960) 507.

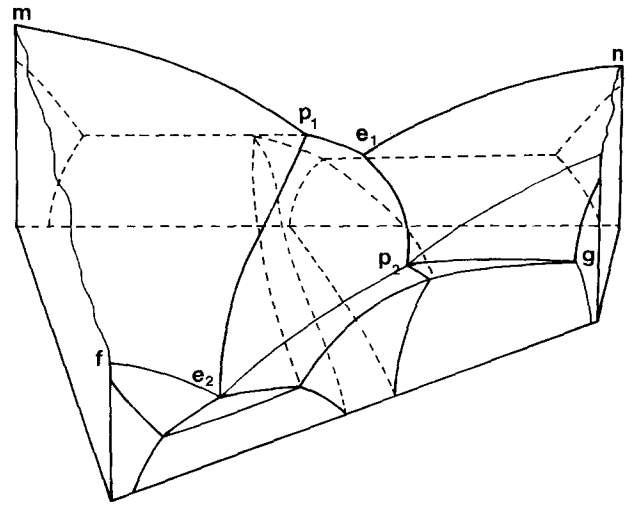

Figure 8 Space representation of eutectic–peritectic monovariant lines.

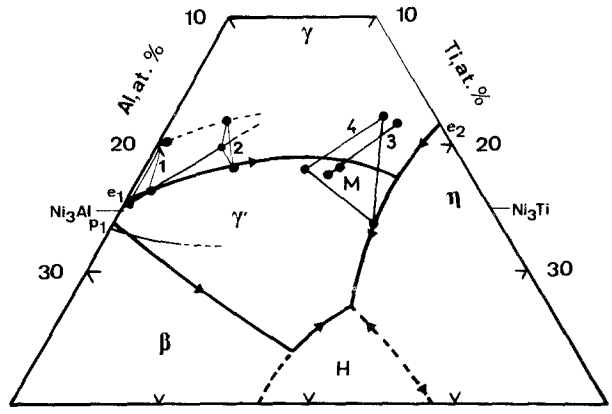

Figure 9 Projected view of tie-triangles illustrating: (1) γ–γ'-liquid eutectic reaction, (2) γ–γ'-liquid peritectic reaction, (3) γ–γ' equilibrium, (4) γ–γ' liquid metatectic reaction.

4. R. S. MINTS, G. F. BELYAYEVA and Y. S. - MALKOV, *Russian Metall.* **2** (1967) 96.
5. P. NASH and W. W. LIANG, *Met. Trans.* **16A** (1985) 319.
6. P. WILLEMIN, O. DUGUE, M. DURAND-CHARRE and J. H. DAVIDSON, *Mater. Sci. Technol.* **2** (1986) 344.
7. P. WILLEMIN, Thèse Doctorat, I.N.P. Grenoble (1986).
8. P. NASH and D. R. F. WEST, *Met. Sci.* **13** (1979) 670.
9. D. BLAVETTE and A. BOSTEL, *Acta Metall.* **32** (1984) 811.
10. M. P. ARBUZOV and I. A. ZELENKOV, *Fiz. Met. Metalloved.* **15** (1963) 725.
11. R. W. GUARD and J. H. WESTBROOK, *Trans. TMS-AIME* **215** (1959) 807.
12. S. OCHIAI, Y. MISHINA and T. SUZUKI, *Bull. Prec. Mach. and Elect.* (*T.I.T.*) **53** (1984).
13. M. MORINAGA, N. YUKAWA, H. ADACHI and H. EZAKI, "Superalloys 1984" edited by Gell *et al.* (Met. Soc. of AIME, 1984) pp. 523–532.

Received 7 June
and accepted 21 October 1988